The interplay between X-ray photoevaporation and planet formation

Giovanni P. Rosotti,[1,2,3]★ Barbara Ercolano,[2,3]★ James E. Owen[4]
and Philip J. Armitage[5,6]

[1]*Max-Planck-Institut für extraterrestrische Physik, Giessenbachstraße, D-85748 Garching, Germany*
[2]*Excellence Cluster Universe, Boltzmannstr. 2, D-85748 Garching, Germany*
[3]*Universitats-Sternwarte München, Scheinerstraße 1, D-81679 München, Germany*
[4]*Canadian Institute for Theoretical Astrophysics, 60 St. George Street, Toronto M5S 3H8, Canada*
[5]*JILA, University of Colorado and NIST, 440 UCB, Boulder, CO 80309-0440, USA*
[6]*Department of Astrophysical and Planetary Sciences, University of Colorado, Boulder, USA*

ABSTRACT

We assess the potential of planet formation instigating the early formation of a photoevaporation-driven gap, up to radii larger than typical for photoevaporation alone. For our investigation we make use of hydrodynamic models of photoevaporating discs with a giant planet embedded. We find that by reducing the mass accretion flow on to the star, discs that form giant planets will be dispersed at earlier times than discs without planets by X-ray photoevaporation. By clearing the portion of the disc inner of the planet orbital radius, planet formation induced photoevaporation (PIPE) is able to produce transition discs that for a given mass accretion rate have larger holes when compared to standard X-ray photoevaporation. This constitutes a possible route for the formation of the observed class of accreting transition discs with large holes, which are otherwise difficult to explain by planet formation or pho-toevaporation alone. Moreover, assuming that a planet is able to filter dust completely, PIPE produces a transition disc with a large hole and may provide a mechanism to quickly shut down accretion. This process appears to be too slow, however, to explain the observed desert in the population of transition discs with large holes and low mass accretion rates.

Key words: accretion, accretion discs – hydrodynamics – protoplanetary discs.

1 INTRODUCTION

The evolution and final dispersal of the gas and dust contained in protoplanetary discs surrounding young low-mass stars plays an important role in shaping the properties of potential planets in the system. In particular the disc dispersal time-scale sets an upper limit for the formation of gas giants. It is therefore crucial to formulate a theory capable of describing the disc evolution and dispersal in detail, which is an important input for the planet formation theory.

For most of their lifetime, the evolution of discs is driven by viscosity. Currently, the most favoured mechanism for its origin is the magnetorotational instability (Balbus & Hawley 1991), although other mechanisms have been proposed, such as the transport of angular momentum by spiral waves in self-gravitating discs (Lodato & Rice 2004). Under simplifying assumptions, the evolution in time of a disc can be described by an analytical solution (Lynden-Bell & Pringle 1974), which was showed to be in rough agreement with the observations (Hartmann et al. 1998) of the mass accretion rates in 'classical' T Tauri discs.

However, the final evolution of protoplanetary discs appears not to be consistent with this picture. Discs have a characteristic lifetime of 3 Myr (Haisch, Lada & Lada 2001; Mamajek 2009; Fedele et al. 2010), as can be seen looking at the fraction of disc-bearing young stellar objects (YSOs) in clusters of different ages, but, rather than from a homogeneous draining as predicted by pure viscosity evolu-tion, discs seem to have a fast, final stage of clearing from the inside out (Luhman et al. 2010; Ercolano, Clarke & Hall 2011; Koepferl et al. 2013) with a typical time-scale of 10^5 yr. This behaviour has been called 'two-time-scale' in the literature.

'Transitional discs' are objects believed to have been caught in the act of disc dispersal and hence believed to be useful for shedding light on the mechanism responsible for disc clearing. Although first spotted by spectral energy distribution (SED) observations of YSOs more than two decades ago (Strom et al. 1989; Skrutskie et al. 1990), only more recently the *Spitzer* space telescope provided the opportunity to study them in detail (e.g. Calvet et al. 2005; Espaillat et al. 2010); they lack emission at the mid-infrared (mid-IR) wavelengths when compared to a 'standard' disc. This deficit in opacity in the warm dust has been interpreted as the signature of an inner hole. SED modelling is, however, a rather difficult task, depending on many model parameters that are often degenerate.

★ E-mail: rosotti@usm.lmu.de (GPR); ercolano@usm.lmu.de (BE)

More recently, the advent of good-quality data from submillimetre interferometers has permitted to obtain spatially resolved images of some of these objects, confirming indeed the presence of large cavities (Andrews et al. 2011), sometimes of the order of tens of au. The frequency of transitional discs (∼10 per cent of the total number of protoplanetary discs) is consistent with the interpretation that they represent a fast, final phase of disc evolution that proceeds from the inside out (Kenyon & Hartmann 1995). It has to be remarked that, despite the images confirm large cavities both in the submillimetre and in the μm-sized dust, gas is in many cases still present. Indeed, some of these transitional discs present mass accretion rates of the order of 10^{-8} M$_{\odot}$ yr^{-1}, comparable with that of classical T Tauri stars, indicating that a substantial reservoir of gas is still present near the central object. Even more remarkably, it has to be noted that such mass accretion rates are not a general feature of all transition discs, and that there is instead a huge range of variation in the observed sample.

To explain the presence of this class of discs, many physical processes have been invoked, including grain growth (Dullemond & Dominik 2005), photoevaporation (Clarke, Gendrin & Sotomayor 2001; Alexander, Clarke & Pringle 2006a) and planet formation (Armitage & Hansen 1999; Rice et al. 2003). However, up to now none of these processes alone has been shown to be sufficient to explain all observations.

Growing through collisions, dust particles can indeed become large enough to become essentially invisible to observations. However, while models of grain growth are able to reproduce the observed dips in their IR SEDs of transitional discs, they predict that the dust should still be visible at millimetric wavelengths, in contrast with what is found in observations (Birnstiel, Andrews & Ercolano 2012).

The presence of a giant planet embedded in the disc is able to open a gap, and acts like a dam, stopping the inflow of matter from the outer disc reservoir. However, the dam is porous, and while the surface density in the inner disc is lowered and the mass accretion rate reduced, the material can still flow towards its way to the star (e.g. Lubow & D'Angelo 2006). To reconcile this with observations, it is necessary to find the right combination of parameters that makes the inner disc optically thin, while still allowing a sensible mass accretion rate. As showed by Zhu et al. (2011), theoretical calculations predict that one single planet is not able to perturb enough the surface density of the inner disc, and multiple accreting planets are required to open a gap of a size consistent with what is found in observations. This reduces, however, the mass accretion rates on to the star as well as the surface density. Zhu et al. (2011) conclude that even in the case of multiple planets it is not possible to interpret discs that exhibit a large hole size together with a high mass accretion rate on to the star.

Photoevaporation is the process through which high-energy radiation (from the central star or from the environment) thermally drives a wind from the disc. The mass-loss rates depend on the detailed physics of the radiation field. Including the effect of extreme-ultraviolet (EUV) radiation from the central star, Clarke et al. (2001) and Alexander, Clarke & Pringle (2006b) showed that the coupled evolution of a viscously evolving disc in the presence of a photo-evaporative wind is able to open a gap in the inner disc when the mass accretion rate through the disc becomes comparable with the mass-loss rate of the wind. Owen et al. (2012) further argue that the dust in the inner disc rapidly drifts on to the star (Alexander & Armitage 2007) – on a time-scale of ∼10^3 yr. The gas drains on its (much longer) viscous time-scale (∼10^5 yr). The result is a disc that exhibits an inner dust cavity (hence a dip in the mid-IR

emission), and an inner gas disc that is still draining, producing a still measurable mass accretion signature. Much progress has been made in computing detailed mass-loss rates from the photoevaporative wind. This is crucial to determine the mass accretion rate at which the wind is able to open a gap, thus determining the age of the disc and the properties of the resulting transition disc. In particular, recent models have included in the calculation far ultraviolet (FUV) and X-ray radiation (Ercolano, Clarke & Drake 2009; Gorti & Hollenbach 2009; Owen, Ercolano & Clarke 2011).

In particular, Owen et al. (2011) compared the statistics of transitional discs with evolution models including X-ray photoevaporation from the central star, showing that it is indeed possible to explain a large number of observed objects with photoevaporation alone. This model, however, still failed to reproduce the class of transitional discs with large holes and large mass accretion rates due to the fact that, by the time photoevaporation has carved a large enough hole in the outer disc, the mass reservoir of the inner disc has dropped so much that no mass accretion rate is detectable anymore.

A possible scenario, as suggested by Owen & Clarke (2012), is that 'transitional' discs are not a homogeneous class, indicating that different physical processes may be at work, and there may be different paths to transitional disc formation, depending on which of these physical mechanisms is dominant. If this is the case, we expect that in some cases there may not be a single dominant process, and it may be the interplay among several of them that leads to a given transitional disc formation.

Along this route, the goal of this paper is to study if the combination of photoevaporation and planet formation, which has been up to now studied separately, can indeed help in interpreting the puzzling population of accreting transitional discs. By reducing the surface density and the mass accretion rate in the inner disc, we expect that the presence of a planet is able to trigger the opening of a gap by photoevaporation at early times. We call this process planet-induced photoevaporation (PIPE). To investigate this scenario, we make use of hydrodynamic models of a photoevaporating disc with a giant planet embedded. Our purpose is to assess how the presence of a planet affects the clearing of the disc by X-ray photoevaporation.

This paper is structured as follows. In Section 2, we present the numerical method we used and the results we obtained. In Section 3, we discuss the results and in Section 4 we draw our conclusions.

2 NUMERICAL INVESTIGATION

2.1 Methods

We study the disc–planet interaction process by means of the 2D grid-based hydrodynamic code FARGO (Masset 2000). The conditions at time t_0 of the formation of the planet are provided by a 1D viscous evolution code, which takes care of evolving the disc from time $t = 0$ to t_0. This allows to save computational resources when detailed evolution of the disc is not needed.

2.1.1 Initial conditions (1D evolution)

As initial conditions, we use the models of Owen et al. (2011). We include the effects of viscous evolution and X-ray photoevaporation. The evolution of the surface density of the disc is described by the following equation:

$$\frac{\partial \Sigma}{\partial t} = \frac{3}{R} \frac{\partial}{\partial R} \left[R^{1/2} \frac{\partial}{\partial R} \left(\nu \Sigma R^{1/2} \right) \right] - \dot{\Sigma}_{\mathrm{w}}(R), \tag{1}$$

where Σ is the surface density, $\dot{\Sigma}_{\mathrm{w}}(R)$ is the photoevaporation profile (as in the appendix of Owen, Clarke & Ercolano 2012) and ν is the kinematical viscosity coefficient, which sets the magnitude of viscosity. We choose the same values of the parameters as in Owen et al. (2011), which we summarize here. We evaluate ν using the α prescription (Shakura & Sunyaev 1973): $\nu = \alpha c_{\mathrm{s}} H$, where c_{s} is the sound speed of the gas, H is the vertical scaleheight and α is the dimensionless Shakura–Sunyaev parameter. In our models, we set $\alpha = 1.5 \times 10^{-3}$. The sound speed is a fixed function of radius, and is chosen to give a mildly flaring disc (i.e. $H/R \propto R^{1/4}$); the normalization is chosen so that at 1 au the aspect ratio $H/R = 0.0333$. Our computational grid covers the range [0.0025 au, 2500 au], and it is comprised of 1000 grid points. The mesh is uniform in a scaled variable $X \propto R^{1/2}$. Our viscous code uses a flux-conserving donor-cell scheme, implicit in time. Details about the implementation can be found in Birnstiel, Dullemond & Brauer (2010).

The initial surface density profile is given by

$$\Sigma(R, 0) = \frac{M_{\mathrm{d}}(0)}{2\pi R R_1} \exp(-R/R_1), \qquad (2)$$

where $M_{\mathrm{d}}(0)$ is the initial mass of the disc and R_1 is the scale radius describing the exponential taper of the disc's outer region. We set a value of $R_1 = 18$ au and an initial disc mass of $0.07\,\mathrm{M}_\odot$.

For what concerns the photoevaporation profile, there are two parameters: the mass of the central star M_* and the X-ray luminosity L_{X}. We chose $M_* = 0.7\,\mathrm{M}_\odot$, while we perform calculations with different values of the X-ray luminosity. We do runs with the median X-ray luminosity $L_{\mathrm{X}} = 1.1 \times 10^{30}\,\mathrm{erg\,s^{-1}}$, which we evolve for 2 Myr before inserting the planet, and runs with a higher X-ray luminosity of $\log L_{\mathrm{X}} = 30.8$, which we evolve for 0.65 Myr. These values for the planet formation time-scale do not come from a physical model, but rather were chosen to have a similar reasonable surface density profile at the moment of the planet formation. Since in the case of high X-ray luminosity the evolution of the disc is faster due to the increased mass-loss rate, we chose a smaller value for the age of the disc at the moment of planet formation. In both cases, the normalization at 1 au is approximately $500\,\mathrm{g\,cm^{-2}}$, which is a factor of 3–4 lower than the minimum mass solar nebula (Hayashi 1981). However, it should be noted that the power-law slope is -1, rather than $-3/2$, so that in the outer region the surface density is higher. The total mass in the disc at the moment of planet formation is approximately $25 M_{\mathrm{J}}$ for the median X-ray luminosity, and 20 for the high X-ray luminosity (the difference is due to the disc being more spread out in the first case), which is higher than the minimum mass solar nebula. We note that according to current planet formation theories, it is difficult, although still plausible (Movshovitz et al. 2010), to form a gas giant in the short time-scale used in the second case; therefore, the high X-ray luminosity case should be regarded as a limiting one.

2.1.2 FARGO *simulations*

At time $t = t_0$, we assume that a gas giant planet forms, and we use the output of the 1D code as input for the 2D FARGO code. We assume that the formation happens on a time-scale fast enough so that we can switch from a 1D disc without a planet to a 2D disc with a planet. The code, which has been widely used in studies of protoplanetary discs, solves the equations of hydrodynamics through finite differences on a grid in cylindrical coordinates. FARGO uses the same algorithms as the ZEUS code (Stone & Norman 1992) for hydrodynamics, but employs a modified azimuthal transport technique that results in a smaller computational request for disc geometries.

The code solves the coupled system of the Navier–Stokes equations and continuity equations. We modified the continuity equation from the publicly available version of the code to include the effects of photoevaporation on the disc. The continuity equation now reads

$$\frac{\partial \Sigma}{\partial t} + \nabla \cdot (\Sigma \boldsymbol{v}) = -\dot{\Sigma}_{\mathrm{w}}(R), \qquad (3)$$

where $\dot{\Sigma}_{\mathrm{w}}$ is the same mass-loss profile due to photoevaporation employed in the 1D evolution. A similar implementation was also used to study planet scattering in transitional discs by Moeckel & Armitage (2012). The removal of mass is done at the beginning of the hydro time-step. To be able to follow the evolution in time of the disc, we implemented a minimum density through the disc. Whenever the density becomes smaller than a given threshold, it is reset to the minimum allowed value. We use the dimensionless value of 10^{-8} for this threshold, which is about five orders of magnitude smaller than the initial value of the density in the disc at the planet location. For safety, we modified also the time-step condition, adding another criterion that does not permit photoevaporation to remove in a single time-step more than a given fraction f of the mass in a cell. We used for f the value of 0.1. However, we noted in our simulations that this condition is never relevant, and that the other usual conditions on the time-step are more restrictive.

We set the parameters to the same values as in the 1D evolution. We are, however, not able to resolve the whole disc in a 2D simulation; therefore, we restrict ourselves in the range $[0.1 r_{\mathrm{p}}, 10 r_{\mathrm{p}}]$, where r_{p} is the planet orbital radius. We employ a resolution of $n_\phi = 256$ cells in the azimuthal direction, uniformly distributed. The radial resolution is then chosen so that each cell is approximately square, which gives $n_r = 188$ cells. While considerably higher resolution simulations can be found in the literature, we remark that here we are interested in the global evolution of the disc, rather than capturing some local property. Even if some feature is not properly resolved (such as the accretion streams on to the planet), this has little effect on the global evolution. For this reason, similar studies of the disc evolution on a long time-scale have employed a resolution similar to ours (e.g., Zhu et al. 2011). We have checked, running simulation M20 at double the resolution and comparing the result, that our results stay the same, with a maximum 10 per cent difference in the mass of the inner disc up to the moment of the disc clearing.

We consider a planet embedded in the disc with a mass $M_{\mathrm{p}} = 10^{-3} M_* = 0.7 M_{\mathrm{J}}$, and we allow the orbital radius of the planet to vary from 10 to 50 au. The planet is not allowed to migrate, although we also performed a run in which we include this effect. In the simulation in which we included also migration, we switched it on only after 500 orbits to restrict to the case of Type II migration and exclude Type I migration. To reduce artefacts in the solutions due to a sudden insertion of the planet, we slowly increase its mass during the first 100 orbits, using the taper function provided in the publicly available version of FARGO. We use open inner boundary conditions and reflecting outer boundary conditions (which is the default in FARGO). To test the impact of this choice, we implemented an open outer boundary condition, finding no significant difference. We use planetary accretion as prescribed by Kley (1999) using the publicly available implementation in FARGO. At each time-step, a fraction of the material inside the Hill radius of the planet is removed and accreted on to the planet. The fraction is controlled by a free parameter, f, that represents the inverse of the accretion time-scale in dynamical units. We use $f = 1$ for our standard model, although we test also a situation with a 10 times slower accretion time-scale. Table 1 summarizes the simulation runs.

Table 1. The table summarizes the simulation runs. The number in the name of the run specifies the position of the planet in au; the 'x' denotes the runs with high X-ray luminosity. In addition to the standard runs, which allow the planet position and the X-ray luminosity to vary, there are also three 'special runs', with the names M20m, M20f and M20o, including migration, with a slower planetary accretion time-scale employed and without photoevaporation. The initial planet mass is in every case $0.7M_{\rm J}$.

Run name	Orbital radius (au)	$\log L_{\rm X}$	t_0 (Myr)	Notes
M10	10	30.04	2	
M20	20	30.04	2	
M20m	20	30.04	2	Migration
M20f	20	30.04	2	Slower accretion
M20o	20	30.04	2	No photoevaporation
M30	30	30.04	2	
M40	40	30.04	2	
M50	50	30.04	2	
M20x	20	30.8	0.65	
M40x	40	30.8	0.65	

Lastly, it should be noted that the inclusion of a photoevaporation profile breaks down the degeneracy of the dimensionless units used by FARGO. In the pure hydrodynamical case, we have one free mass scale and the results can then be scaled to different central star masses. This is no longer the case including photoevaporation, because $\dot{\Sigma}_{\rm w}$ depends on the (physical) radius in the disc and on the mass of the star.

2.2 Results

2.2.1 Qualitative picture

The surface density in the disc at three different times from runs M20 and M20o is plotted in Fig. 1. In the left-hand panel, at an age of approximately 2.1 Myr, the dynamical gap cleared by the planet is evident, but photoevaporation has not yet started to clear the disc. The surface density at this stage is very similar to a control run without photoevaporation; the most notable differences are visible at the gap edges. The planet acts like a dam for the viscous flow, reducing the mass accretion rate in the inner part of the disc. This permits photoevaporation to take over, and clear the inner disc, as
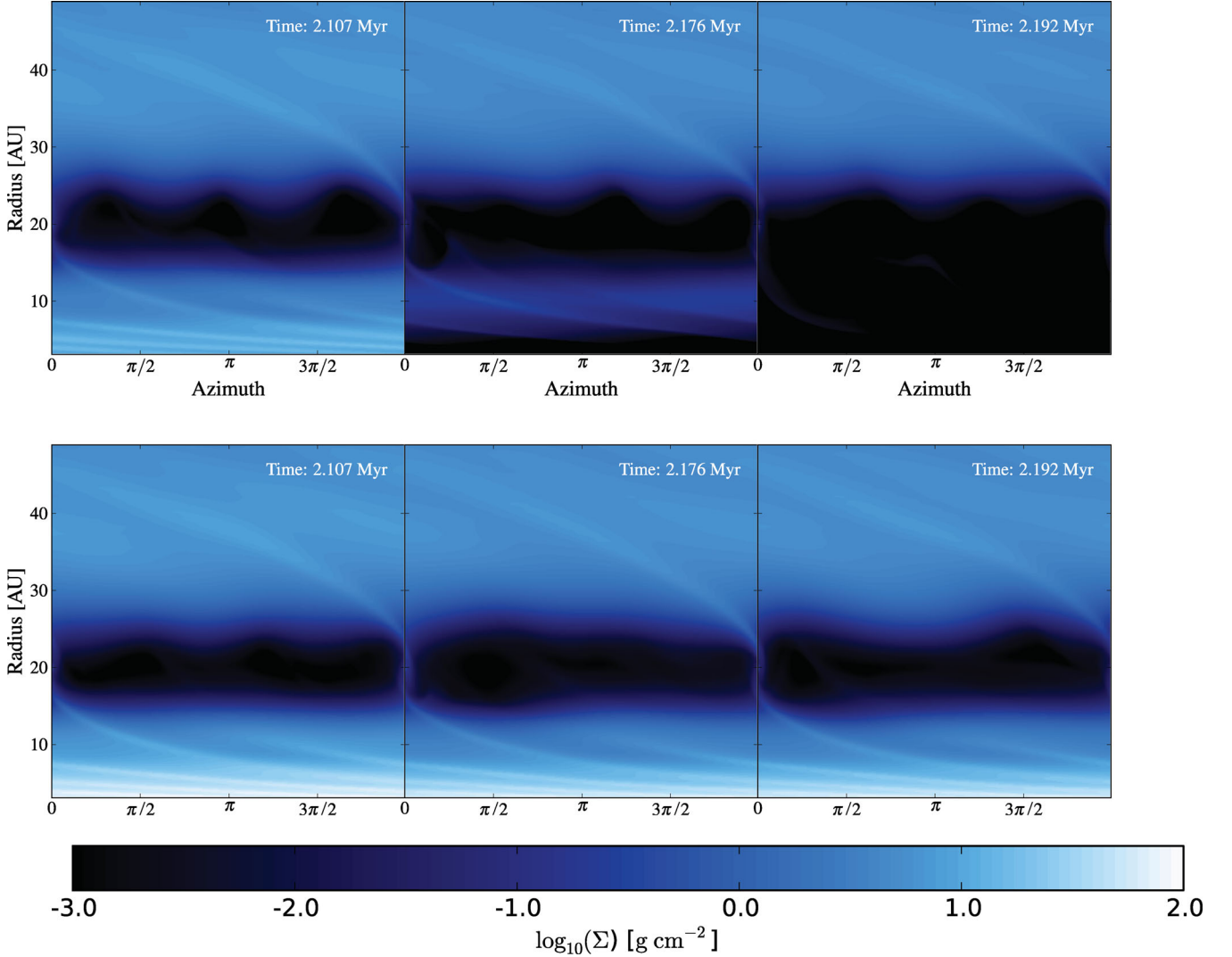
Figure 1. Top row: surface density in the disc at three different times from simulation M20. Bottom row: same quantities for simulation M20o, which do not include photoevaporation. While in the first snapshot the inner disc is still there also in the case of photoevaporation included, it is caught in the act of clearing in the second snapshot. Finally, we are left with a disc with the outer part only in the last snapshot. In the control simulation, instead, the inner disc is left.
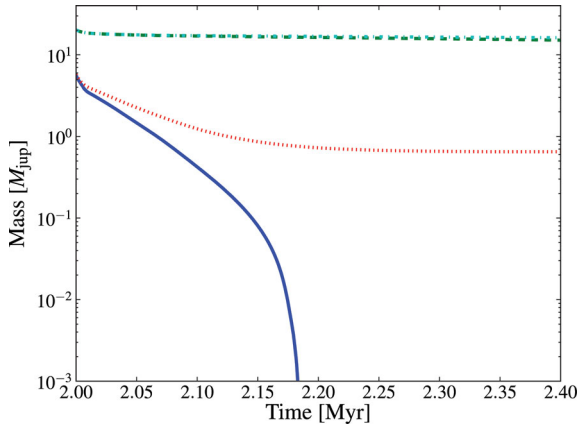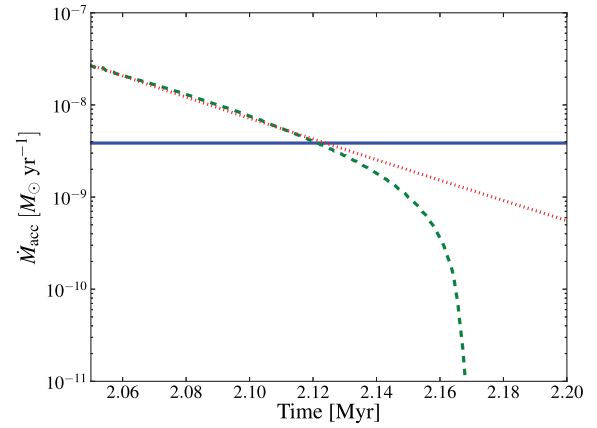
Figure 2. Solid blue line: mass of the inner disc (i.e. inside the planet orbital radius) with photoevaporation (run M20). Dotted red line: mass of the inner disc without photoevaporation (run M20o). Dashed green line: mass of the outer disc (i.e. outside the planet orbital radius) with photoevaporation (run M20). Dot–dashed cyan line: mass of the outer disc without photoevaporation (run M20o). In run M20 with photoevaporation, the inner disc is rapidly dissipated, while in the control run M20o it reaches a sort of steady-state value.
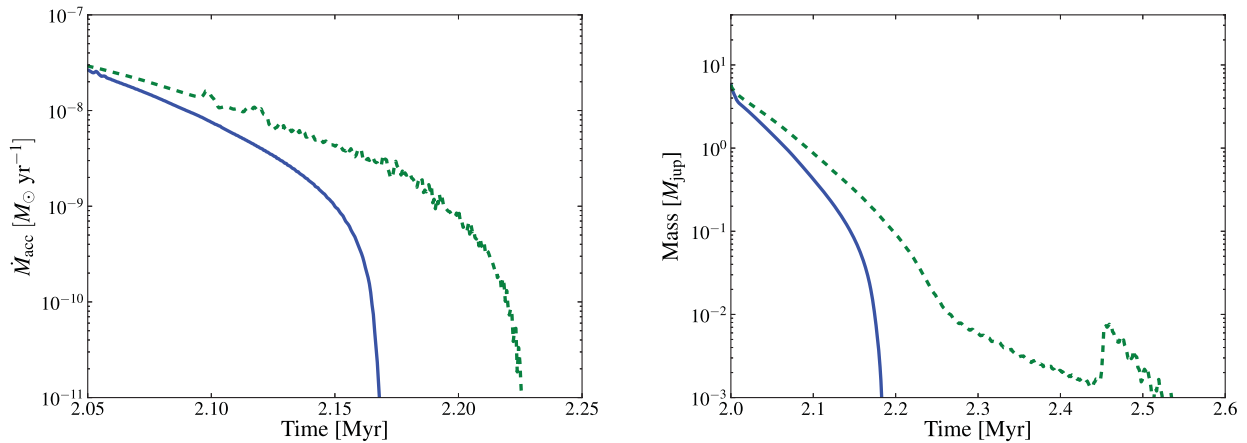

Figure 3. Green dashed line: mass accretion rate at the inner boundary of the grid as a function of time for simulation M20. For reference, the blue solid horizontal line shows the mass-loss rate due to photoevaporation in the inner disc, while the red dotted line is a straight line added as a visual aid to distinguish the moment of the inner disc clearing. The change in the slope of the mass accretion rate corresponds to the inner disc clearing. This clearing happens when the mass accretion rate has dropped below some factor of the mass-loss rate.

can be seen in the intermediate step in which photoevaporation is clearing the disc from inside out. Finally, we are left only with the outer disc, when the disc is approximately 2.2 Myr old. It should be noted that the clearing of the inner disc is due to the combined effect of photoevaporation and planet formation. In the control simulation M20o without photoevaporation, the mass of the inner disc is reduced, but not cleared completely, as can be seen from the bottom row of Fig. 1. On the other hand, with photoevaporation alone the disc would have cleared on a longer time-scale, after 3.3 Myr. It can be concluded that PIPE, i.e. the combined effects of photoevaporation and planet formation, is able to clear the inner disc at earlier times, that is, stars with giant planets will dissipate their inner discs quicker.

Fig. 2 shows the masses of the outer and inner discs (i.e. at radii larger and smaller than the planet orbital radius) as a function of time. For reference we included also the result of the control run M20o without photoevaporation. While they start from the same initial value, the difference accumulates in time, and when photoevaporation becomes important it rapidly dissipates the inner disc. In contrast, in the control run without photoevaporation, the mass of the inner disc reaches some kind of steady-state value, slightly smaller than a Jupiter mass. Due to our use of a floor density, after the clearing of the inner disc there is still a non-zero mass inside the orbit of the planet, with a value that is around $10^{-4}M_{\rm J}$ (out of scale in the figure). It should be noted also that there is little difference in the mass of the outer disc between the two runs, and that the final value is around $15M_{\rm J}$.

In Fig. 3 we plot the mass accretion rate at the inner boundary of the grid. The change in the slope corresponds to the moment at which the inner disc starts to clear. In the figure, we overplot also, as a horizontal line, the mass-loss rate due to photoevaporation (considering the inner disc only). It can be seen that only once the mass accretion rate has dropped below some factor of the mass-loss rate the clearing begins. The qualitative understanding of disc clearing is thus not really different from the evolution of a disc without a planet, namely the two-time-scale behaviour (as in the UV switch model): for most of its lifetime the evolution of the disc is driven by viscosity, and only when the mass accretion rate

drops below the mass-loss rate due to photoevaporation the clearing begins. The role of the planet is that of accelerating this process, acting like a dam that reduces the mass accretion rate in the inner disc. We remark that, since the inner disc spends most of its lifetime with a mass accretion rate that is higher than the mass-loss rate, the total mass of the disc that has been lost through accretion is greater than the one carried away by photoevaporation. Thus, it is the accretion that does most of the 'dirty job' of dissipating the disc, and photoevaporation only contributes in the last step of the removal. For what concerns planetary accretion, we have checked that most of the mass that ends up on the planet comes from the outer disc. This does not mean that planetary accretion does not play a role in the dispersal of the inner disc. Indeed, it controls the porosity of the planetary dam, fixing the amount of the viscous flow from the outer disc that is intercepted. This effect makes the mass of the planet increase by a factor of 6 at the moment of disc dispersal. However, the direct effect, namely the mass accreted by the planet directly from the inner disc, is little compared with the mass leaving the grid from the inner boundary, apart from a small initial transient in which the planet is accreting from the region that will be dynamically cleared.

2.2.2 *Effect of the planet accretion time-scale*

This qualitative picture implies that a crucial parameter for estimating the impact of the presence of a planet in the disc is the porosity of the dam. We notice that in a 1D simulation the planet acts as a complete dam, and no filtering is possible. Thus, one has to insert by parametrization the porosity of the dam (e.g., Alexander & Armitage 2009), in a way that does not conserve angular momentum. This effect is better accounted for in 2D simulations, where the transport of angular momentum across the gap is treated in a realistic fashion, although there is still a dependence on the planet accretion time-scale. To test how robust our results are with respect to the variation of this parameter, we run a simulation with a 10 times higher value (i.e. the planet accretes 10 times slower), $f = 10$, that we call M20f. In the left-hand panel of Fig. 4, we propose a comparison between the mass accretion

Figure 4. Left-hand panel: comparison of the mass accretion rate at the inner boundary as a function of time, varying the planetary accretion time-scale. The blue solid line is for the standard value ($f = 1$), run M20, and the green dashed line for the slow accretion ($f = 10$), run M20f. Right-hand panel: comparison of the mass of the inner disc as a function of time. The lines have the same style as in the left-hand panel.

rate at the inner boundary of the grid of this simulation with the standard one. The inner disc is indeed cleared at later times, since we need to wait more for the mass accretion rate to drop, due to the higher porosity of the dam. However, it should be noted that the difference is not so dramatic as one could expect by such a big variation in the time-scale. This is consistent with what other authors have found, namely that the process of planetary accretion is not dramatically dependant on the value of this parameter (Kley 1999). What cannot be seen from this plot, however, is that the way in which the disc clears is different. This can be seen from the mass of the inner disc versus time comparison in the right-hand panel of Fig. 4. We can see that with a reduced planetary accretion time-scale not only the clearing happens at later times, but it is also slower. Visual inspection of the surface density distribution shows that an inner ring of material is left just inside the orbit of the planet, which is only slowly eroded. We interpret this as due to the fact that, because of the higher mass accretion rate through the planetary gap, photoevaporation has a much more difficult job at removing this part of the disc, being continuously replenished from the outer disc. This shows the complex structures that may be formed due to the interplay between the different physical processes acting in the disc.

2.2.3 Varying planet position

In the simulation shown so far, the planet has a semi-major axis of 20 au. To find how the inner disc clearing depends on the planet position, we ran other simulations with different values of this physical parameter. Fig. 5 shows a comparison in the mass of the inner disc (normalized to the initial value) as a function of time for the different simulation runs, with the planet position varying from 10 to 50 au (runs M10–M50). The farther out the planet is, the slower is the process of dispersal. This is expected, since more time is required for a farther out planet to reduce the mass accretion rate near the star. However, we can see that in all cases the disc dispersal is considerably faster than without the presence of a planet in the disc. A fit to the initial surface density profile with equation (2) gives for R_1 a value of approximately 80 au, so that for the used values of the planet position the planet is able to cut most of the disc mass reservoir from the inner radii. From this argument we expect that a planet farther out than R_1, if able to form, would not have a significant impact on the disc lifetime.
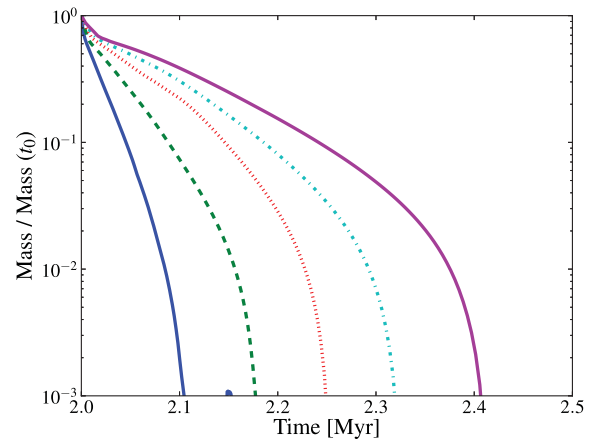

Figure 5. Comparison of the mass of the inner disc normalized to the initial value for simulations with different positions of the planet, varying from 10 to 50 au (runs M10–M50). The farther the planet, the slower the clearing of the disc.

2.2.4 Varying X-ray luminosity

As a limiting case, we run simulations with a high value of X-ray luminosity equal to $\log L_X = 30.8$. The disc is 0.65 Myr old at the time when the giant planet is inserted. While this may sound like an unrealistically young age for planet formation, we note that the relative disc age can be obtained by the appropriate scaling of initial parameters and here we chose a value that gives a similar surface density normalization (although the disc is less spread, being younger) to the previous case. This shows how even quite a massive disc can be rapidly dispersed by the combined effect of X-ray photoevaporation and planet formation.

The evolution of the mass of the inner disc as a function of time, normalized to the initial value, is shown in Fig. 6 for different values of the planet initial position. Because of the higher mass-loss rates of photoevaporation, everything is happening quicker, with a dispersal that can happen so fast as less than 10^5 yr after the planet formation. Also in this case, the farther the planet, the slower the process of disc dispersal. Visual inspection of the images confirms the same qualitative behaviour we outlined in the previous section.
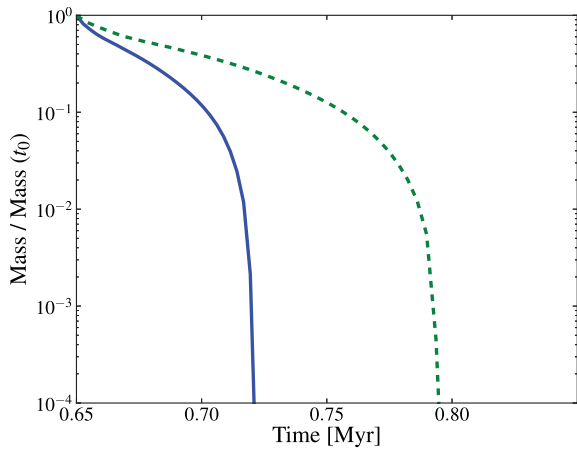
Figure 6. Mass of the inner disc, normalized to the initial value, as a function of time, for simulations with a high value of the X-ray luminosity with the positions of the planet at 20 and 40 au, runs M20x (solid blue line) and M40x (dashed green line).

2.2.5 Effect of migration

To test the sensitivity of our results to migration, that we neglected so far, we run a simulation with migration included, M20m. The left-hand panel of Fig. 7 shows a comparison in the masses of the inner disc, showing that there is very little difference in the process of disc clearing. This is a consequence of the fact that the clearing proceeds from inside out, so that the beginning of the clearing is set by the properties of the disc in the inner portion, rather than in the neighbourhood of the planet that is affected by migration. The right-hand panel of Fig. 7 shows the semi-major axis as a function of time, showing that the planet has not migrated much before the disc is dispersed, approximately 2 au. It may be argued that this is a consequence of the initial conditions, namely that we took quite an evolved disc. Inserting the planet at earlier times would have allowed more time to migrate, and therefore to be more incisive in modifying the clearing. This is what has been studied by Alexander & Armitage (2009) and Alexander & Pascucci (2012), who coupled the disc evolution to the planet migration and studied the resulting planet distribution. The effect of more massive planets inserted in massive (self-gravitating) discs is the focus of a forthcoming study

by Clarke et al. (in preparation), while in this work we focus on the study of less massive disc–planet systems.

3 DISCUSSION

In the previous section, we showed how PIPE is able to change the picture of disc dispersal with respect to photoevaporation or planet formation alone. The main finding is that discs with a planet are likely to be dispersed earlier than discs without. An interesting test of the PIPE scenario is to compare its predictions with the observations of transitional discs that are interpreted as discs caught in the act of clearing. In particular, we study the $\dot{M}$–R_{hole} parameter space. For each of our models, the aim is to compute evolutionary tracks that can be plotted in this parameter space. In contrast with Owen et al. (2011), due to the increased computational cost, we are not able to run here a whole population synthesis; rather, we will be limited to comparing with individual data points. In particular, we wish to answer the question if transition discs with large holes and mass accretion rates can be accounted for by PIPE. A similar attempt has been made by Morishima (2012) through the modelling of X-ray photoevaporating discs with dead zones.

Unfortunately, our hydrodynamical modelling does not yield directly these parameters. In particular, the mass accretion rate the observations measure is the one on to the star, which we cannot resolve for numerical reasons. Therefore, we make two limiting assumptions to the modelling.

In the first, conservative assumption, we assume that the X-ray photoevaporation driven clearing of the innermost disc proceeds as it would do in the absence of a planet, opening a gap at approximately 1.5 au. This gap is inside the region that we can resolve in the simulation. The disc will then exhibit two gaps, the dynamical one cleared by the planet and the one opened by photoevaporation, that divide the disc in three distinct regions (named A, B and C in the following for clarity). As in the photoevaporation case, we assume that the dust in the innermost disc A will drain very quickly ($\sim 10^3$ yr) on to the star, so that region A will be invisible in observations. The disc will then look like a transition disc and the radius of the hole is set by the inner radius of disc B, that we can measure from the 2D simulation. While A is draining, there is still a measurable mass accretion rate. We assume that the dependence on time of the mass accretion rate on to the star is the same as in the 1D simulation, where we take as the beginning of clearing the
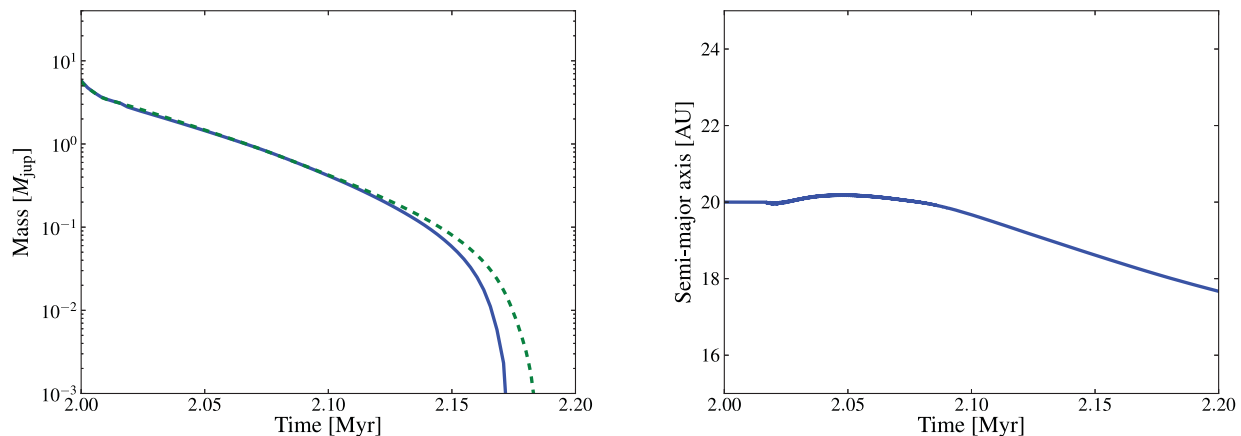

Figure 7. Results from simulation M20m including migration. Left-hand panel: the mass of the inner disc as a function of time for simulation M20m (blue solid line). For reference has been plotted also the case without migration, run M20 (green dashed line). Right-hand panel: semi-major axis of the planet as a function of time.
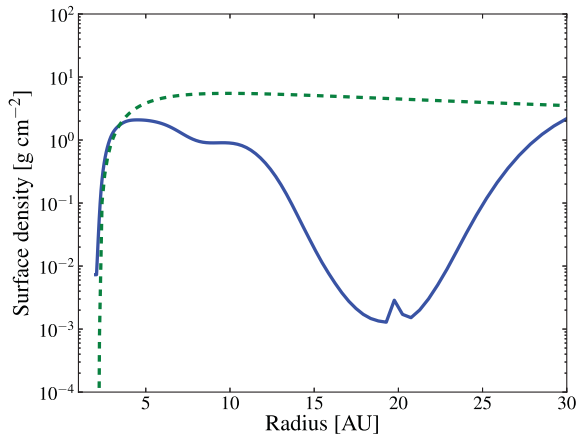
Figure 8. Surface density as a function of radius just before the inner disc clearing starts in run M20 (blue solid line), compared with the surface density in the 1D calculations from the Owen et al. (2011) model with the median X-ray luminosity (green solid line). The surface densities are quite similar near to the inner boundary, while at greater radii, in the case with a planet the surface density profile is much flatter.

time at which in the 1D simulation the radius of the hole is the inner boundary of our 2D grid. We note that the density structure in the region we can resolve is quite similar before the onset of clearing of the inner disc, as we show in Fig. 8. In this figure, we compare the surface density from our FARGO simulation M20 just before the inner disc begins to clear with the results from the 1D run without the planet, at the time in which the radius of the hole is 2 au (namely the inner radius of our 2D grid). The surface densities near the inner boundary are very similar, while at larger radii the density distribution is lower, due to the presence of the planet that makes this region devoid of gas. This motivates us to assume that the dependence on time of the mass accretion rate on to the star is the same as in the case without the planet, coming from the draining of the disc A on to the star, but now with a different R_{hole} dependence that is derived from the 2D simulation. In Fig. 9 we compare the R_{hole} dependence for model M20 and for the corresponding model without
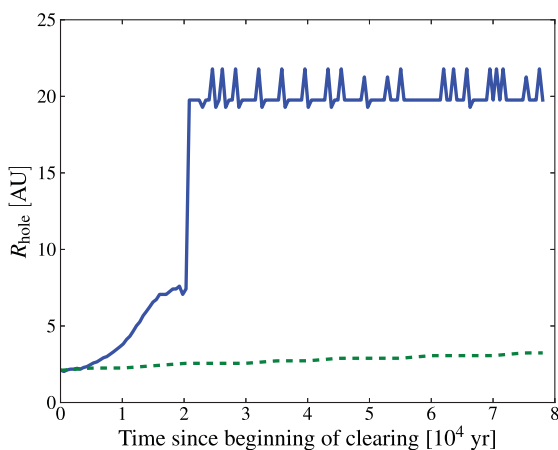
Figure 9. Inner hole radius a function of time (since the clearing), for the PIPE M20 calculation (blue solid line) and the 1D model with the median X-ray luminosity (green dashed line) from Owen et al. (2011). The depletion of the surface density caused by the planet makes the opening of the hole much faster. The oscillations that can be seen in the radius of the hole in model M20 are a consequence of the oscillations at gap edges visible in Fig. 1.
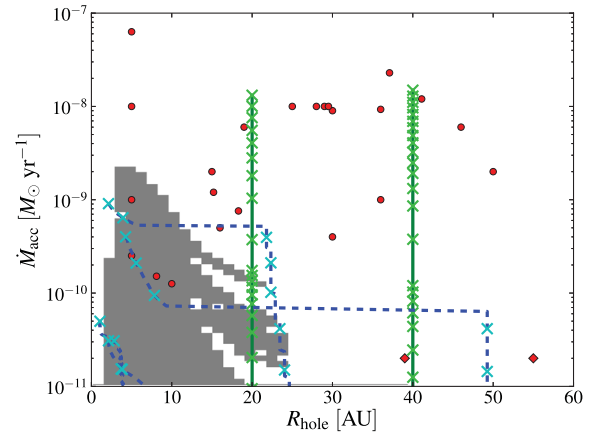
Figure 10. $\dot{M}$–R_{hole} parameter space of transition discs. The grey area is the area permitted by X-ray photoevaporation alone, as in Owen et al. (2011). The points are the observed data points with high millimetre flux from Owen & Clarke (2012). The diamonds are for discs without a detected mass accretion rate. The blue dashed tracks are for the first assumption (see text) and the green continuous tracks are for the second; the crosses on the tracks are plotted every 10^4 yr.

a planet, i.e. the Owen et al. (2011) model with the median X-ray luminosity. We define the radius of the hole simply as the minimum radius where the azimuthally averaged surface density is above the imposed floor density (with an allowance factor of 10, due to the presence of numerical oscillations above the floor density). Because of the mentioned depletion of the surface density, the clearing of the hole is much faster in the case with photoevaporation. When compared to models that include X-ray photoevaporation alone, we thus expect PIPE models to yield higher mass accretion rates for the same hole size, or conversely larger holes at the same mass accretion rate. The time $t = 0$ in the plot refers to the beginning of the clearing, and it is the one when in the 1D simulation the radius of the hole is 2 au. We plot our results in the $\dot{M}$–R_{hole} parameter space in Fig. 10 as the blue dashed tracks. The cyan crosses are plotted every 10^4 yr. Runs M20x and M40x are the ones that produce the higher mass accretion rates, while only runs M10 and M20 are visible from the runs with the median X-ray luminosity. The points in the plot are the observed data points that exhibit a high millimetre flux, as it is described in Owen & Clarke (2012). The data points show a weak correlation between the hole radius and the mass accretion rate, which has not been explained yet. The grey area is the area permitted by X-ray photoevaporation alone, as in Owen et al. (2011). Using this conservative assumption (blue lines), one would then conclude that the PIPE scenario is indeed able to expand the parameter space with respect to photoevaporation alone, but that the mass accretion rates obtained are still too low compared with the observations.

The other limiting assumption, which is a best case scenario for us, is the one in which the planet is able to filter the dust, so that the disc would look like in transition, even if there is still a huge quantity of gas inside the orbit of the planet. In synthesis, by modifying the surface density profile of the disc, the planet creates a pressure maximum. Dust particles, flowing inwards, are unable to cross this maximum, so that the dust is filtered out from the inner portion of the disc, which becomes invisible to observations. This simple picture is complicated by the other dust processes that happen simultaneously (coagulation, fragmentation, diffusion, . . .). This process has been studied in detail by Rice et al. (2006), Pinilla, Benisty & Birnstiel (2012) and Zhu et al. (2012). In this case, we take the orbital radius

of the planet as the radius of the hole. Before the clearing starts, we take the mass accretion rate at the inner boundary of the grid, starting from 500 orbits since the beginning of the simulation (to exclude initial oscillations), under the assumption that the mass accretion rate in the inner portion of the grid that we do not simulate is set by the outer part that we can resolve. Once the inner disc starts to clear, we take as in the previous case the mass accretion rate as predicted by the case without the planet. The resulting tracks in this case (plotted in the green continuous lines in Fig. 10) look like vertical lines, since there is little evolution of the radius during the simulation, and the mass accretion rate simply decreases. Using this second assumption, one would then conclude that, when the dust properties are taken into account, PIPE is able to explain discs with large holes and mass accretion rates. While up to now the theoretical effort has been to predict whether the appearance of a planet-bearing disc resembles that of transitional discs, little work has been done in understanding the evolution of such systems. Photoevaporation could potentially give a reason for the shutting down of accretion, which is requested from the lack of observed data points in the region of the plot with large holes and low mass accretion rates. To explore this possibility, we plotted light-green crosses along the tracks every 10^4 yr. There is not, however, a clear separation between the uppermost and the lower parts of the track, with only a little jump that is not enough to account for the desert on the observed desert in the observed distribution. If this desert is real and not due to observational biases (e.g. discs with high mass accretion rates are also more massive), then a new mechanism must destroy the outer disc. Such a mechanism could be given by the 'thermal sweeping' effect, an instability found in photoevaporating discs with an inner hole by Owen et al. (2012), able to destroy the disc in the order of the dynamical time-scale. The forthcoming work of Clarke et al. (in preparation) presents an alternative scenario based on the carving of millimetre-bright accreting transition discs by massive planetary companions embedded and migrating in self-gravitating discs.

Our results suggest that the interplay between X-ray photoevaporation and planet formation is worthy of further study. Our work also implies that planets are an important ingredient in the disc dispersal process, and should be included in the modelling. The ability of the upcoming ALMA facility will be hopefully able to tell more about the gas structure in transitional discs, which is at the moment very poorly constrained.

3.1 Model limitations

In this paper, it has been assumed that the photoevaporation profile is the same as computed by Owen et al. (2011), who modelled the photoevaporative flow in a disc without a planet. Large-scale 3D simulations that include both photoevaporation and a planet embedded are being carried out and will be presented in a forthcoming paper (Rosotti et al., in preparation).

The absolute time-scales discussed in the paper should be taken with caution as they strongly depend on a number of simplifying assumptions. First of all, a source of uncertainty comes from an unknown mechanism for angular momentum transport. In this work, we have considered a simple α-disc and assumed a constant value of α. The assumption of a constant α-value is common in many theoretical studies of discs (e.g. Alexander, Clarke & Pringle 2006b; Gorti, Dullemond & Hollenbach 2009; Owen et al. 2011), and is motivated by a lack of strong observational constraints, and for simplicity, it is necessary to isolate the effect of other processes that affect the evolution of the disc. However, no known theory of angu-

lar momentum transport predicts a constant value for α (Armitage 2011). Therefore, such an assumption should be regarded more as a matter of convenience. Studies addressing the issue of how a physical model for viscosity, e.g. the layered accretion model proposed by Gammie (1996), changes the evolution of the disc have been conducted by, for example, Armitage et al. (2002) and Morishima (2012). The layered accretion model predicts the formation of dead zones in the disc, where the viscosity is significantly lower than in the active parts of the disc. This is due to the insufficient ionization level in the cold mid-plane of the disc, which is not enough to couple the gas with the magnetic field and trigger the magnetorotational instability. The accretion continues in a thin layer, where the ionizing radiation (X-rays from the star and cosmic rays) is able to penetrate. The net effect, once vertically averaged, is to create a zone with a reduced viscosity. Employing a different model of photoevaporation from the one used in this paper, Armitage et al. (2002) modelled the combined evolution of a giant planet migrating in a layered disc. They find that the main effect of layered accretion is to slow down planetary migration due to the longer viscous time-scale. However, as showed in Section 2.2.5, migration is already relatively unimportant for our results, so this is probably a second-order effect. Morishima (2012) found that the interplay between dead zones and photoevaporation can also be a possible route for the formation of transition discs with large holes and large mass accretion rates. Their results predict that, near the outer edge of a dead zone, the radial motion of gas is directed outwards, while it is inwards inside the dead zone region. This effect, once coupled with photoevaporation, may be able to open a gap in the disc at the outer edge of the dead zone, around 40 au in their calculations. The dead zone in the inner disc will survive for a long time after the opening of a gap, so that $\dot{M}$ remains high even after the gap opens. Such considerations may also apply to the systems explored in this work. It is, however, difficult to predict the effect of a varying viscosity induced by the presence of a dead zone on the disc clearing time-scales calculated here. The location and extent of the supposed dead zone with respect to the planet will have a strong influence on how the dispersal is affected. Even the direction of the feedback from dead-zone formation is difficult to predict. On the one hand, a dead zone reduces the mass accretion rates in the region, hence reducing the mass flows through a planet gap, yielding to a faster decoupling of the inner and outer discs. However, if the dead zone contains most of the disc mass, as in the Morishima (2012) calculations, its effect could also be one of stabilization of the mass accretion rates in the inner disc, resulting in a slower draining of the latter. Clearly a focused exploration of the relevant parameter space would be required in order to provide educated predictions of the interaction of dead zones (or indeed variable viscosity) with PIPE, which is beyond the scope of this work. Further uncertainties in the absolute time-scales are introduced by numerical limitations, in particular the under-resolution of the inner boundary that influences the resulting inner disc clearing time-scales. Experiments have shown that the effect of having an inner boundary at a larger radius is to produce a higher mass accretion rate at the beginning of the simulation. This makes the disc deplete faster, thus shortening the lifetime of the disc. Therefore, while a faster disc evolution due to the combined effect of photoevaporation and planet formation is a robust prediction of PIPE (as can be seen by comparison of Fig. 1), absolute disc lifetimes may be longer than what presented here. While this effect is irrelevant for the first assumption presented here in the discussion, it could partially help in explaining the mentioned desert in the observed transitional disc population. In addition, as already said in the previous sections, this numerical

limitation precluded us the possibility of following the evolution of the very inner disc, where photoevaporation is opening a gap.

Finally, another possible improvement of the models presented here is adding the modelling of the dust, in order to be able to compare directly the outcome of the model with observations. This will be particularly important to compare with ALMA observations.

4 CONCLUSIONS

In this paper, we presented results from 2D simulations of discs with giant planets embedded undergoing X-ray photoevaporation. Our results show that planet formation influences the process of disc dispersal by photoevaporation. The main consequences of PIPE can be summarized as follows:

(i) By reducing the mass accretion flow on to the star, discs that form planets will be dispersed at earlier times by X-ray photoevaporation than discs without planets.

(ii) For what concerns transitional discs, PIPE is able to produce transition discs that for a given mass accretion rate have larger holes when compared to standard X-ray photoevaporation. However, further modelling of the dust processes is needed to be able to fully exploit the observational consequences of this process.

(iii) Assuming that the planet is able to filter dust completely (Rice et al. 2006; Pinilla et al. 2012; Zhu et al. 2012), large hole transition discs could be produced. PIPE may instigate the shutting-down accretion; however, our simplified models cannot at present explain the observed desert in the population of transition discs with large holes and low mass accretion rates.

REFERENCES

Alexander R. D., Armitage P. J., 2007, MNRAS, 375, 500
Alexander R. D., Armitage P. J., 2009, ApJ, 704, 989
Alexander R. D., Pascucci I., 2012, MNRAS, 422, L82
Alexander R. D., Clarke C. J., Pringle J. E., 2006a, MNRAS, 369, 216
Alexander R. D., Clarke C. J., Pringle J. E., 2006b, MNRAS, 369, 229
Andrews S. M., Wilner D. J., Espaillat C., Hughes A. M., Dullemond C. P., McClure M. K., Qi C., Brown J. M., 2011, ApJ, 732, 42
Armitage P. J., 2011, ARA&A, 49, 195
Armitage P. J., Hansen B. M. S., 1999, Nat, 402, 633
Armitage P. J., Livio M., Lubow S. H., Pringle J. E., 2002, MNRAS, 334, 248
Balbus S. A., Hawley J. F., 1991, ApJ, 376, 214
Birnstiel T., Dullemond C. P., Brauer F., 2010, A&A, 513, A79
Birnstiel T., Andrews S. M., Ercolano B., 2012, A&A, 544, A79
Calvet N. et al., 2005, ApJ, 630, L185
Clarke C. J., Gendrin A., Sotomayor M., 2001, MNRAS, 328, 485
Dullemond C. P., Dominik C., 2005, A&A, 434, 971
Ercolano B., Clarke C. J., Drake J. J., 2009, ApJ, 699, 1639
Ercolano B., Clarke C. J., Hall A. C., 2011, MNRAS, 410, 671
Espaillat C. et al., 2010, ApJ, 717, 441
Fedele D., van den Ancker M. E., Henning T., Jayawardhana R., Oliveira J. M., 2010, A&A, 510, A72
Gammie C. F., 1996, ApJ, 457, 355
Gorti U., Hollenbach D., 2009, ApJ, 690, 1539
Gorti U., Dullemond C. P., Hollenbach D., 2009, ApJ, 705, 1237
Haisch K. E. Jr, Lada E. A., Lada C. J., 2001, ApJ, 553, L153
Hartmann L., Calvet N., Gullbring E., D'Alessio P., 1998, ApJ, 495, 385
Hayashi C., 1981, Prog. Theor. Phys. Suppl., 70, 35
Kenyon S. J., Hartmann L., 1995, ApJS, 101, 117
Kley W., 1999, MNRAS, 303, 696
Koepferl C. M., Ercolano B., Dale J., Teixeira P. S., Ratzka T., Spezzi L., 2013, MNRAS, 428, 3327
Lodato G., Rice W. K. M., 2004, MNRAS, 351, 630
Lubow S. H., D'Angelo G., 2006, ApJ, 641, 526
Luhman K. L., Allen P. R., Espaillat C., Hartmann L., Calvet N., 2010, ApJS, 186, 111
Lynden-Bell D., Pringle J. E., 1974, MNRAS, 168, 603
Mamajek E. E., 2009, in Usuda T., Tamura M., Ishii M., eds, AIP Conf. Ser. Vol. 1158, Exoplanets and Disks: Their Formation and Diversity. Am. Inst. Phys., New York, p. 3
Masset F., 2000, A&AS, 141, 165
Moeckel N., Armitage P. J., 2012, MNRAS, 419, 366
Morishima R., 2012, MNRAS, 420, 2851
Movshovitz N., Bodenheimer P., Podolak M., Lissauer J. J., 2010, Icarus, 209, 616
Owen J. E., Clarke C. J., 2012, MNRAS, 426, L96
Owen J. E., Ercolano B., Clarke C. J., 2011, MNRAS, 412, 13
Owen J. E., Clarke C. J., Ercolano B., 2012, MNRAS, 422, 1880
Pinilla P., Benisty M., Birnstiel T., 2012, A&A, 545, A81
Rice W. K. M., Wood K., Armitage P. J., Whitney B. A., Bjorkman J. E., 2003, MNRAS, 342, 79
Rice W. K. M., Armitage P. J., Wood K., Lodato G., 2006, MNRAS, 373, 1619
Shakura N. I., Sunyaev R. A., 1973, A&A, 24, 337
Skrutskie M. F., Dutkevitch D., Strom S. E., Edwards S., Strom K. M., Shure M. A., 1990, AJ, 99, 1187
Stone J. M., Norman M. L., 1992, ApJS, 80, 753
Strom K. M., Strom S. E., Edwards S., Cabrit S., Skrutskie M. F., 1989, AJ, 97, 1451
Zhu Z., Nelson R. P., Hartmann L., Espaillat C., Calvet N., 2011, ApJ, 729, 47
Zhu Z., Nelson R. P., Dong R., Espaillat C., Hartmann L., 2012, ApJ, 755, 6

This paper has been typeset from a T_EX/L^AT_EX file prepared by the author.